ARTICLES

Band approach to the excitation-energy dependence of x-ray fluorescence of TiO_2

L. D. Finkelstein, E. Z. Kurmaev, and M. A. Korotin
Institute of Metal Physics, Russian Academy of Sciences, Ural Division, 620219 Yekaterinburg, GSP-170, Russia

A. Moewes
CAMD/LSU, Baton Rouge, Louisiana 70803

B. Schneider
Universitat Osnabrück, Fachbereich Physik, D-49069 Osnabrück, Germany

S. M. Butorin
Institute of Metal Physics, Russian Academy of Sciences, Ural Division, 620219 Yekaterinburg, GSP-170, Russia and Physics Department, Uppsala University, Box 530, S-75121 Uppsala, Sweden

J-H. Guo and J. Nordgren
Physics Department, Uppsala University, Box 530, S-75121 Uppsala, Sweden

D. Hartmann and M. Neumann
Universitat Osnabrück, Fachbereich Physik, D-49069 Osnabrück, Germany

D. L. Ederer
Department of Physics, Tulane University, New Orleans, Louisiana 70118

(Received 9 February 1999)

Excitation-energy dependence of Ti $L_{2,3}$ soft x-ray emission spectra (XES) of a TiO_2 single crystal is measured near Ti $2p$ threshold using tuneable synchrotron radiation at excitation energies $E_{exc} = 458.2-476.9$ eV. It is found that the emission spectra exhibit normal soft x-ray emission features, which do not change with excitation energy and inelastic and resonant x-ray emission features (RXES), which strongly depend on the excitation energy. We are using a band approach in order to discuss the excitation-energy dependence of Ti $L_{2,3}$ RXES of TiO_2. The RXES process is described as a convolution of occupied and unoccupied d states in the intermediate and final states. In this procedure the d states are limited to those which lie in the energy interval $E_{exc} \pm \Delta E$ taking into account the rule of k conservation. We calculate the curves of restricted joint density of states using the full potential linearized muffin-tin orbital method and the results are found to be in reasonable agreement with the experimental Ti $L_{2,3}$, RXES of TiO_2 measured at different excitation energies. [S0163-1829(99)12227-6]

I. INTRODUCTION

The soft x-ray emission spectra excited by tunable synchrotron radiation near the threshold reveal additional features compared to those measured at excitation energies far above threshold.[1] The former spectra are often called resonant x-ray emission spectra (RXES) and the latter are called normal x-ray emission spectra (NXES). The presence of one *elastic peak* and one or more *inelastic peaks* is a typical peculiarity of RXES. All these features shift on an *emission energy* scale with changes in excitation energy and the energy position of the *elastic peak* indicates excitation energy E_{exc}.

RXES spectra are interpreted in the framework of different approaches. One approach, based on the d-d multiplet of a free atom, is found to be successful for the interpretation of RXES of $3d$ and $4f$ compounds, such as, for instance, MnO (Ref. 2) and lanthanides.[3] RXES of strongly covalent $3d$ and $4f$ compounds, such as TiO_2, CeO_2, and PrO_2 are analyzed by means of a cluster approach or the Anderson impurity model which allows us to form a structure of the final state using interacting multielectron configurations and independent parameters.[4–6] Despite some schematic character of such approaches, the obtained set of energy levels of the final state reproduces the structure of excited levels of the initial state of the system. This approach is developed in Ref. 7 by expansion of the size of the cluster and takes into account nonlocal excitations in the intermediate state of the process. In Refs. 8 and 9 the inelastic region of Ti $L_{2,3}$ RXES of TiO_2 is attributed to soft x-ray inelastic scattering and the corresponding energy loss has its origin in an excitation of an electron from the valence band to the conduction band. In

this paper we interpret the data with the band approach. Even the direct comparison of Ti $L_{2,3}$ RXES with Ti $3d$ density of states (DOS) distribution shows their qualitative agreement though it seems to be more correct to compare Ti $L_{2,3}$ RXES with restricted joint density of states (rJDOS) which is a convolution of vacant $3d$ DOS in the narrow energy interval $E_{\rm exc} \pm \Delta E$ with occupied $3d$ DOS. Among the occupied $3d$ valence states we select only those quasi-impulses which correspond to k values which lead to an excited state in the conduction band in the energy interval $E_{\rm exc} \pm \Delta E$. In this way we obey the k-conservation rule for optical transitions between the valence and conduction band.

II. EXPERIMENTAL AND COMPUTATIONAL DETAILS

Ti $L_{2,3}$ XES and O $K\alpha$ XES of a TiO_2 single crystal were measured at the undulator beamline 7.0 of the ALS, Lawrence Berkeley Laboratory with a spherical grating monochromator[10] using an end station with grating spectrometer described in Ref. 11 and at beamline 8.0 using the Rowland circle grating end station.[12] High-resolution grazing-incidence grating spectrometers with a two-dimensional detector were utilized to measure x-ray fluorescence. Spectrometer resolution was about 0.8 eV. For energy calibration of Ti $L_{2,3}$ XES and O $K\alpha$ XES, the spectra of reference samples Ti, V, and MgO were measured. In order to determine the excitation energies, absorption spectra at the Ti $2p$ and O $1s$ edges were measured at the 90° incidence angle by means of total electron yield (TEY) and with a monochromator resolution set to about 0.2 eV. The x-ray fluorescence and absorption spectra were brought to a common energy scale using an elastic peak in the fluorescence spectra recorded at the excitation energy set below the absorption edge.

The x-ray photoelectron spectroscopy (XPS) measurements have been carried out with a PHI 5600 ci ESCA using monochromatized Al $K\alpha$ radiation of 0.3 eV full width at half maximum (FWHM). The energy resolution of the analyzer was 1.5% of the pass energy. We estimate the energy resolution of the spectrometer to be less than 0.35 eV for the XPS measurements. The pressure in the vacuum chamber during the measurements was below 5×10^{-9} mbar. The TiO_2 single crystal was cleaved in ultrahigh vacuum for XPS measurements in order to analyze surfaces without contaminations. All the measurements were made at room temperature. The XPS spectra were calibrated using the Au $4f_{7/2}$ signal from a Au foil. The binding energy $E_{\rm BE}$ for the Au $4f_{7/2}$ electrons is 84.0 eV.

Band structure calculations of TiO_2 were performed for rutile crystal structure using the full potential linearized muffin-tin orbital (FP LMTO) method.[13,14] The tetragonal structure of the rutile crystal belongs to the D_{4h}^{14} space group and contains two formula units in the elemental cell with lattice parameters $a = 4.5936$ A, $c = 2.9587$ A.[15] Eight empty spheres (ES) in $8i(0.3840, 0.1248, 0.0)$ positions were added to two titanium atoms in $2a(0,0,0)$ positions and four oxygen atoms in $4f(0.3048, 0.3048, 0)$ positions for more dense packing of the unit cell. $R_{\rm Ti} = 1.023$ A, $R_{\rm O} = 0.923$, $R_{\rm ES} = 0.781$ Å atomic sphere radii were used in the present calculation. The basis included Ti $4s4p3d$, O $2s2p$ and ES $1s,2p$ valence orbitals. The procedure of self-consistency has been carried out on 405 k points in an irreducible Brillouin zone. The obtained results of band structure calculation are in agreement with those of Ref. 16.

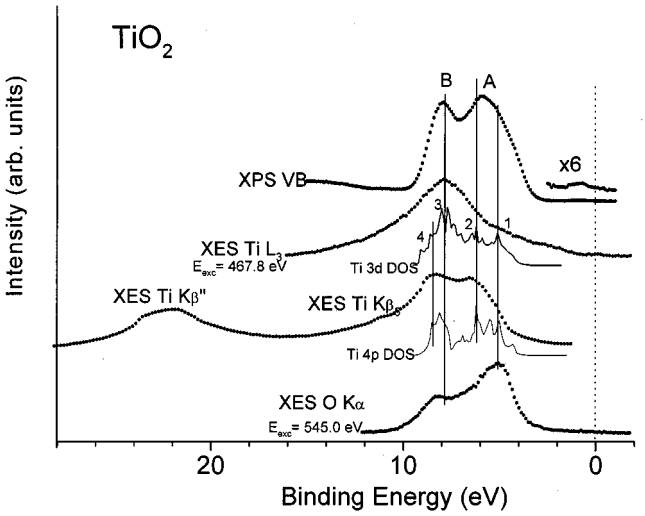

FIG. 1. Comparison of experimental XPS VB, Ti L_3 XES, Ti $K\beta_5$ XES (Ref. 17), and O $K\alpha$ XES and Ti $3d$, Ti $4p$ DOS on binding energy scale.

III. RESULTS AND DISCUSSION

We will start the discussion of our experimental spectra with the analysis of the XPS valence band (VB), which probes a total density of states distribution in the valence band. The XPS VB of TiO_2 measured at 0–16 eV is shown in Fig. 1. In order to discuss the origin of the main peaks A and B, we have compared this spectrum with Ti L_3 XES ($3d4s \rightarrow 2p_{3/2}$ transition), Ti $K\beta_5$ XES ($4p \rightarrow 1s$ transition), and O $K\alpha$ XES ($2p \rightarrow 1s$ transition). These transitions probe, in accordance with dipole selection rules, partial Ti $3d4s$, Ti $4p$, and O $2p$ DOS, respectively, in the valence band of TiO_2 (see Fig. 1). Ti L_3, Ti $K\beta_5$, and O $K\alpha$ XES are converted to the binding energy scale using our measured XPS binding energies of core levels: $E_{\rm BE}({\rm Ti}\ 2p_{3/2}) = 459.1$ eV, $E_{\rm BE}({\rm O}\ 1s) = 530.6$ eV, $E_{\rm BE}({\rm O}\ 2s) = 22.3$ eV. Ti $K\beta_5$ XES of TiO_2 was taken from Ref. 17 and compared with the XPS VB by alignment of energy position of the Ti $K\beta''$ subband with XPS O $2s$ band. The partial Ti $3d$ and Ti $4p$ DOS are compared with experimental spectra in the binding energy scale by alignment of the main maximum of the $3d$ DOS with the corresponding experimental Ti L_3 XES peak.

According to our band structure calculations (Fig. 2), the O $2p$ DOS is higher than Ti $3d$ DOS along the whole valence band of TiO_2. On the other hand, according to Ref. 18, the O $2p$ atomic photoionization cross section is also higher than that of Ti $3d$ for $E = 1486$ eV (Al $K\alpha$). Therefore, one can expect approximately an equal ratio of the intensities of the two peaks A and B in the XPS VB and O $K\alpha$ XES. However, as seen from Fig. 1 I_B/I_A is higher for the XPS VB than for O $K\alpha$. This indicates that Ti $3d$ states give a noticeable contribution to the formation of the B peak of the XPS VB of TiO_2. It is necessary to point out that some asymmetry of the A peak of the XPS VB is apparently due to d contri-

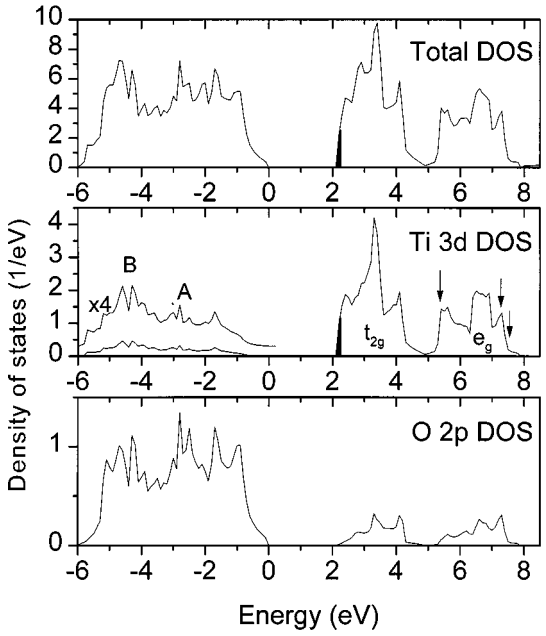

FIG. 2. Total and partial density of states for TiO_2 (total DOS per unit cell; partial DOS per atom). Shaded region of the conduction band corresponds to $TiO_{1.95}$ composition. Arrows indicate three levels 5.3, 7.2, and 7.5 eV corresponding to $E_{exc}=459.9$, 467.8, and 468.9 eV for experimental Ti $L_{2,3}$ XES.

bution from maximum 2 of Ti $3d$ DOS (see Fig. 1). Thus, the energy position of peaks *A* and *B* of the XPS VB gives us information about the location of two main peaks of Ti $3d$ DOS. It is interesting that the main maximum of Ti $4p$ DOS is shifted in respect to that of Ti $3d$ DOS both in experiment and in calculation (Fig. 1). The same conclusion can be drawn for the energetic position of the Ti $4s$ DOS (not shown in Figs. 1 and 2) with respect to that of Ti $3d$ DOS. Ti $4sp$ DOS is placed close to peak 4 of Ti $3d$ DOS.

Analysis of intensity distribution of the XPS VB at 0–1 eV (near the Fermi level) on an enlarged scale ($\times 6$) reveals the existence of a weak peak centered at ~ 0.7 eV. In the XPS VB of a reduced sample of TiO_2 this peak is seen without any enlargement (see Ref. 19) and coincides in energy with the Ti $3d$ peak of the XPS VB of Ti_2O_3.[8] Most likely this peak has an impurity character and is connected with the presence of oxygen defects. The energy difference between this peak and the main peak of Ti $3d$ DOS is about 6.6 eV. We will show later that both peaks contribute to the formation of Ti $L_{2,3}$ RXES of TiO_2.

Results of a FP LMTO band structure calculation of TiO_2 are presented in Fig. 2, zero of the energy scale corresponds to the top of the valence band. The shaded area of the conduction band indicates a position of the Fermi level for $TiO_{1.95}$ which simulates the presence of some oxygen vacancies. $TiO_{1.95}$ is equivalent to composition $Ti_{1.025}O_2$, and it is assumed that the oxygen deficiency is accompanied by occupancy of the bottom of the conduction band by *d* electrons of 2.5% additional Ti atoms. We note in passing that the distance between the bottom of the conduction band and the main peak *B* of Ti $3d$ DOS of the valence band is about 6.6 eV, which is exactly the value derived from XPS VB measurements. Apparently a gap is formed between impurity level and conduction band in this case because the compound is an insulator, but such a situation cannot be reproduced by band structure calculation. After excitation from the initial state ($2p^6$ VB), the excited electron and the core hole take part in the formation of an intermediate state ($2p^5$ VB CB^{+1}) from which the emission transition to the final state ($2p^6$ VB) takes place (VB and CB stand for conduction and valence band, respectively.) As we have already pointed out, the electronic structure of the system in the initial state (in our case Ti $3d$ DOS) can be considered as an adequate ''image'' of the final state for the resonance emission. However, the intensity of the Ti *L* RXES is determined by not only Ti $3d$ DOS of the final state but also by that of the intermediate state. The variation of Ti $3d$ DOS in the intermediate state is reproduced by Ti $2p$ x-ray absorption spectroscopy (XAS).

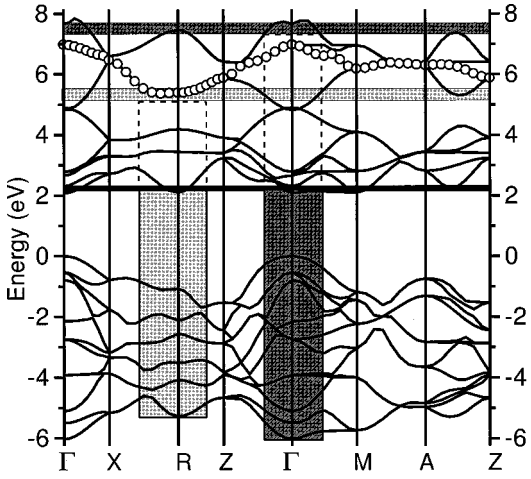

FIG. 3. $E(k)$ dispersion curves for TiO_2. Zone N 24 is shown by open circles. Thick line indicates level of filling for $TiO_{1.95}$ composition. Horizontal shaded areas simulate two excitation levels $E_{exc}=5.3\pm0.2$ and 7.5 ± 0.2 eV from the top of the valence band.

In optical/vacuum ultraviolet (VUV) spectroscopy the intensity of transitions between the valence band and conduction band are described by the joint density of states (JDOS). In the RXES process only some regions of the conduction band participate, depending on the excitation-energy range $E_{exc}\pm\Delta E$ (where ΔE is the accuracy of E_{exc}) and the restricted joint density of states should be used. The formation of JDOS and rJDOS is realized by obeying the *k*-conservation rule. In our case this means that emission transitions take place only in regions of the Brillouin zone which accept E_{exc}.

The dispersion curves $E(k)$ are shown in Fig. 3. The horizontal bars correspond to different excitation energies and the width of the bars indicates the accuracy in the excitation energy E_{exc} ($E_{exc}\pm0.2$ eV). The zone N 24 (counted from the bottom of the valence band) is indicated by open circles in Fig. 3. The vertical bars correspond to the symmetry ranges in which the energy losses take place. For instance, at $E_{exc}=5.3$ eV the vacant states of this zone are only excited near the *R* point. Therefore in the convolution process not all states of the valence band have to be taken into account.

Figure 4 shows Ti $L_{2,3}$ soft x-ray emission spectra measured at excitation energies near the Ti $2p$ threshold. The

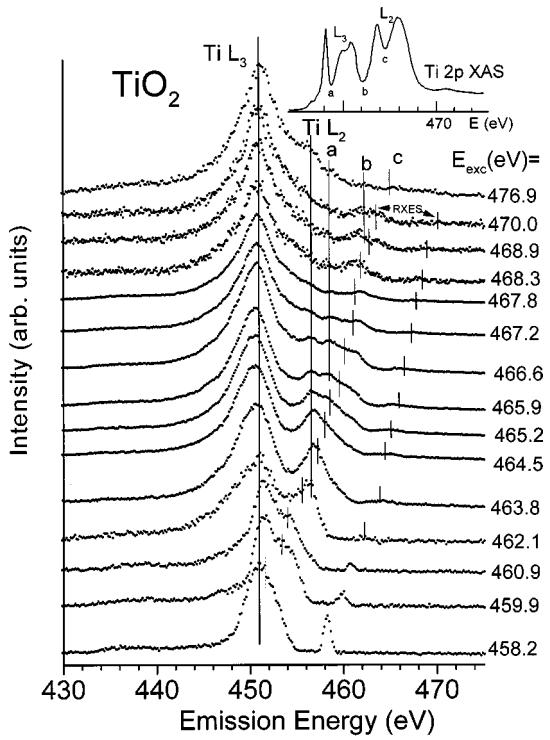

FIG. 4. Excitation-energy dependence of Ti $L_{2,3}$ XES of TiO_2. The upper panel shows Ti $2p$ XAS of TiO_2. The thick solid line indicates energy position of Ti $L2$ and $L3$ NXES. The short vertical lines correspond to the energy loss which appears at 6.6 eV below the elastic peak.

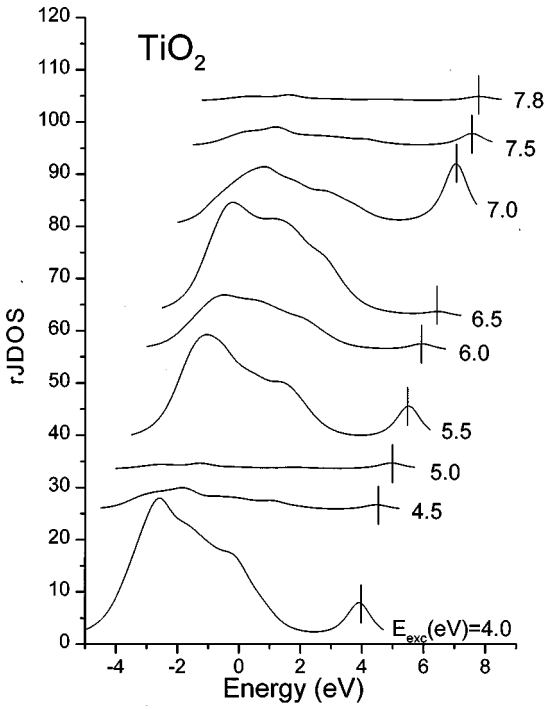

FIG. 5. Ti $3d$ rJDOS of TiO_2 calculated for different energies which imitate experimental E_{exc}. Zero of energy scale corresponds to the top of the valence band.

spectra contain Ti L_3 NXES and Ti L_2 NXES which are indicated by the two solid vertical lines and weak features *a*, *b*, and *c*. The emission energies corresponding to the peaks *a*, *b*, *c* are indicated as *a*, *b*, *c* in the absorption spectrum (XAS) in Fig. 4. We suppose that *a*, *b*, *c* in the emission are induced by weakening of the self-absorption effect at these energies. The spectra exhibit the normal emission (Ti $L_{2,3}$) peaks, elastic peaks at emission energies equal to the excitation energy and inelastic features at about ~6.6 eV below the elastic peak. Similar effects were observed in Refs. 4, 8, and 9. Ti L_3 RXES is shifted with E_{exc} and its intensity is varied according to the fine structure of Ti L_3 XAS, which reflects the probability of excitation of a Ti $2p$ photoelectron to the levels of the intermediate configuration $2p^5 3d^1$. At $E_{\mathrm{exc}} = 462.1$ eV, which corresponds to the minimum between Ti L_3 XAS and Ti L_2 XAS, the Ti L_2 emission is switched on via the inelastic process because the inelastic scattering evolves into this fluorescence peak. The intensity of Ti L_2 RXES is considerably less than that of Ti L_3 RXES due to higher probability of radiationless decay of the $2p_{1/2}^5 3d^1$ state. When the Ti L_2 threshold of ionization is reached (at 465 eV), the intensity of Ti L_2 NXES is decreasing and beginning from $E_{\mathrm{exc}} = 467.8$ eV it completely disappears. Ti L_2 NXES appears again when the excitation energy at $E_{\mathrm{exc}} = 476.9$ eV exceeds the region of *d* states of Ti $2p$ XAS. The intensity decreasing of $3d$ metal L_2 NXES is usually attributed to radiationless Coster-Kronig transition. But why is it especially strongly realized when E_{exc} exceeds the L_2 threshold of ionization for 3–5 eV? We suggest that the Auger electron arising as a result of Coster-Kronig transition receives from the system not only energy for relaxation of the L_2 to L_3 hole but also kinetic energy of photoelectron ionizing the L_2 level. Their total energy is about 8.5–10.5 eV, which is in agreement with energy difference between occupied part of Ti $3d$ DOS and two vacant *d* bands (Fig. 2). It seems that a transition of the Auger electron to vacant states with high density increases the probability of Auger process and suppresses the radiative transition. At $E_{\mathrm{exc}} = 465.9$–467.2 eV, when Ti L_2 NXES still exists but is rather weak, the structure, which is connected with self-absorption, is well defined. This structure is less seen on the slope of strong Ti L_2 NXES and completely absent at $E_{\mathrm{exc}} = 467.8$ eV when Ti L_2 NXES does not present.

The spectrum measured at $E_{\mathrm{exc}} = 467.8$ eV gives information about the shape of Ti L_2 RXES free from the influence of Ti L_2 NXES and *a* structure. The further increasing of E_{exc} leads to the appearance of an additional intensity at energies less than the limit of the 6.6 eV interval marked for Ti L_2 RXES. The energy position of the new line coincides with a *b* feature which is connected with self-absorption. In the absence of this line the self-absorption effect will not exceed the *b* structure at $E_{\mathrm{exc}} = 476.9$ eV.

The nine curves selected from the rJDOS calculated for an interval of excitation energies at 4.0–7.8 eV from the top of the valence band are presented in Fig. 5. These energies imitate experimental E_{exc} and the shift of energy peaks imitates the change of emission energy of inelastic and elastic peaks of experimental spectra. For calculation of rJDOS we have performed a convolution of *d* DOS of the intermediate and final state, i.e., *d* density of the conduction band in the limits of excitation energy $E_{\mathrm{exc}} \pm \Delta E$ is weighted for the *d*-state distribution in the valence band taking into account

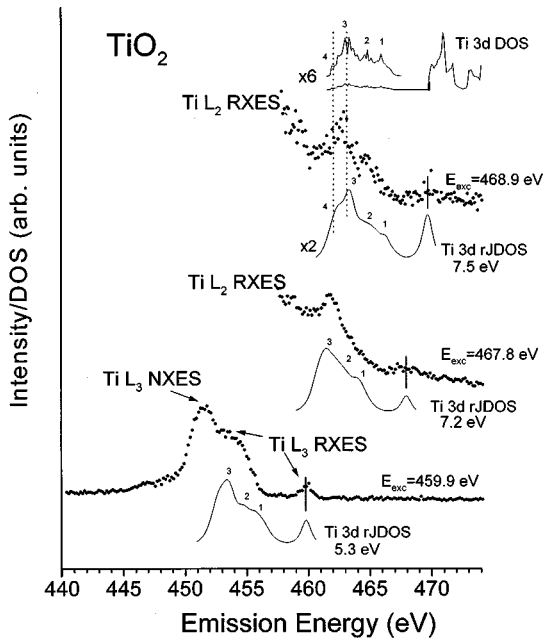

FIG. 6. Comparison of experimental Ti $L_{2,3}$ XES of TiO_2 measured at selected excitation energies with corresponding Ti $3d$ rJDOS. Ti $3d$ DOS is compared with RXES measured at 468.9 eV by alignment of impurity level with elastic peak.

the k-conservation rule. ΔE is taken as 0.2 eV, which indicates the energy uncertainty of the incident photon.

The comparison of three experimental RXES with calculated rJDOS is given in Fig. 6. We have chosen experimental RXES measured at $E_{\mathrm{exc}}=459.9$, 467.8, and 468.9 eV which are less influenced by superposition of NXES spectra. Three energy regions with width of 0.4 eV of the vacant $3d(e_g)$ DOS centered at $E=5.3$, 7.2, and 7.5 eV (from the top of the valence band) correspond to given values of E_{exc} and simulate intermediate states for resonance emission. They are indicated in Fig. 2 by arrows. rJDOS curves are compared with RXES by alignment of the elastic peak energy.

As shown in Fig. 6, the rJDOS calculations reproduce the energy interval between the elastic peak and the main inelastic peak 3 and their relative intensities as well as the appearance of an additional inelastic structure 4 at an excitation energy of 468.9 eV. At this energy the electron is excited to the top of the conduction band. Ti $3d$ DOS is compared with rJDOS calculated for 7.5 eV in the upper panel of Fig. 6 by alignment of energy of the d-impurity level at the bottom of the conduction band. This comparison clearly shows that the elastic peak reflects the d-impurity level, which plays the role of the ground state of the system because it is a low level of ionization and the set of weakly resolved inelastic peaks 1–4 corresponds to distribution of $3d$ states in the O $2p$-like valence band. Therefore a picture of the final state of emission reproduces the energy distribution of Ti $3d$ DOS of the initial state. A variation of intensity between selected RXES for different excitation energies reflects the change of unoccupied d density and also k dependence of rJDOS. Particularly the appearance of structure 4 of rJDOS for 7.5 eV is due to excitation in the vicinity of the Γ point forming DOS on the bottom of the valence band (see Fig. 3). An impurity d level is revealed in RXES considerably stronger than in the XPS VB and NXES because it strengthens in the process of the convolution at the expense of density of unoccupied d states.

IV. CONCLUSION

In this paper we have used a band approach to interpret our measurements of Ti $L_{2,3}$ spectra of resonance x-ray emission of TiO_2. The excitation interval $E_{\mathrm{exc}}\pm\Delta E$ ($\Delta E=0.2$ eV) in the conduction band is used as an intermediate state. The final state of emission is simulated by distribution of $3d$ DOS in the valence band. The emission process is described as convolution of d states of the intermediate and final states taking into account the k-conservation rule. We find reasonable agreement when we compare the calculated rJDOS curves with selected experimental RXES spectra.

ACKNOWLEDGMENTS

This work was supported by the Russian Science Foundation for Fundamental Research (Project Nos. 96-15-96598 and 98-02-04129), NATO Linkage Grant (Grant No. HTECH.LG 971222), the DFG-RFFI Project, the Swedish Natural Science Research Council (NFR), and the Göran Gustavsson Foundation for Research in Natural Sciences and Medicine.

[1] J. Nordgren and N. Wassdahl, Phys. Scr. **T31**, 103 (1990).
[2] S. M. Butorin, J.-H. Guo, M. Magnuson, P. Kuiper, and J. Nordgren, Phys. Rev. B **54**, 1 (1996).
[3] M. Nakazawa, H. Ogasawara, A. Kotani, and P. Lagarde, ISSP Technical Report No. ISSN 0082-4798, Ser. A, No. 3920, 1997 (unpublished).
[4] S. M. Butorin, J.-H. Guo, M. Magnuson, and J. Nordgren, Phys. Rev. B **55**, 4242 (1997).
[5] S. M. Butorin, D. C. Mancini, J.-H. Guo, N. Wassdahl, J. Nordgren, M. Nakazawa, S. Tanaka, T. Uozumi, A. Kotani, Y. Ma, K. E. Myano, B. A. Karlin, and D. K. Shuh, Phys. Rev. Lett. **77**, 574 (1996).
[6] S. M. Butorin, L.-C. Duda, J.-H. Guo, N. Wassdahl, J. Nordgren, M. Nakazawa, and A. Kotani, J. Phys.: Condens. Matter **9**, 8155 (1997).
[7] T. Ide and A. Kotani, ISSP Technical Report No. ISSN 0082-4798, Ser. A, No. 3407, 1998 (unpublished).
[8] Y. Tezuka, S. Shin, A. Agui, M. Fujisawa, and T. Ishii, J. Phys. Soc. Jpn. **65**, 312 (1996).
[9] J. Jimenez-Mier, J. Van Ek, D. L. Ederer, T. A. Callcott, J. J. Jia, J. Carlisle, L. Terminello, A. Asfaw, and R. C. C. Perera, Phys. Rev. B **59**, 2649 (1999).
[10] H. A. Padmore and T. Warwick, J. Synchrotron Radiat. **1**, 27 (1994), and references therein.
[11] J.-H. Guo, N. Wassdahl, P. Skytt, S. M. Butorin, L.-C. Duda, C. J. Englund, and J. Nordgren, Rev. Sci. Instrum. **66**, 1561 (1995);

and J. Nordgren, G. Bray, S. Gramm, R. Nyholm, J.-E. Rubensson, and N. Wassdahl, *ibid.* **60**, 1690 (1989).
[12] J. J. Jia, T. A. Callcott, J. Yurkas, A. W. Ellis, F. J. Himpsel, M. G. Samant, J. Stöhr, D. L. Ederer, J. A. Carlise, E. A. Hudson, L. J. Terminello, D. K. Shuh, and R. C. C. Perera, Rev. Sci. Instrum. **66**, 1394 (1995).
[13] M. Methfessel, Phys. Rev. B **38**, 1537 (1988).
[14] M. Methfessel, C. O. Rodriguez, and O. K. Andersen, Phys. Rev. B **40**, 2009 (1989).
[15] S. C. Abrahams and J. L. Bernstein, J. Chem. Phys. **55**, 3206 (1971).
[16] S.-Di Mo and W. Y. Ching, Phys. Rev. B **51**, 13 023 (1995).
[17] M. A. Blokhin and A. T. Shuvaev, Izv. Akad. Nauk SSSR, Ser. Fiz. **26**, 429 (1962).
[18] J. J. Yeh and I. Linday, At. Data Nucl. Data Tables **32**, 1 (1985).
[19] Z. Zang, S.-P. Jeng, and V. E. Henrich, Phys. Rev. B **43**, 12 004 (1991).